High Temperatures-High Pressures, Vol. 50, pp. 149–165
Reprints available directly from the publisher
Photocopying permitted by license only
DOI: 10.32908/hthp.v50.1013

Metal-carbon eutectic high temperature fixed points for in-situ calibration of radiation thermometers

G. Failleau*, N. Fleurence, O. Beaumont, R. Razouk, J. Hameury and B. Hay

Laboratoire National de métrologie et d'Essais, 29 avenue Roger Hennequin, 78197 Trappes, France

Received: July 8, 2020; Accepted: August 28, 2020.

The diffusivimeter of LNE has been modified by improving the inductive furnace used to heat the tested specimens in order to extend the operating temperature range up to 3000 °C. The temperature of specimen is one of the tricky parameters to be measured to ensure the relevance of the thermal diffusivity measurement and the associated uncertainty. At high temperature, radiation thermometers are used to determine the temperature of the specimens at which the thermal diffusivity measurements are performed. In addition to the periodic calibration of the radiation thermometers performed outside the experimental facility with black body sources, LNE proposes an in-situ verification method based on miniature high temperature fixed-point cells filled with metal-carbon eutectic alloys in order to detect and correct potential drift of the radiation thermometers between two *out-of-process* calibration operations. The proposed method enables high repeatable and reproducible temperature measurements on eutectic fixed-points (Pd-C, Pt-C and Ir-C) distributed in the range from 1500 °C to 2300 °C.

Keywords: Thermal Diffusivity, High Temperature, Radiation Thermometry, Fixed-Point

*Corresponding author: guillaume.failleau@lne.fr

1 INTRODUCTION

LNE has performed for many years thermal-diffusivity measurements of solid materials up to 2000 °C by using a homemade facility based on the principle of the laser-flash method [1]. In this method, a cylindrical specimen, maintained at a constant temperature in a furnace, is heated on one face by a short energy pulse and the transient temperature rise induced on the other face is measured versus time. The thermal diffusivity is determined using an estimation procedure based on minimizing the difference between the experimental temperature-time curve (thermogram) obtained and the same curve given by a theoretical model describing the transient heat conduction through the specimen.

This metrological facility has been modified in the framework of the European joint research project Hi-TRACE [2] by improving the inductive furnace used in order to extend the operating temperature range up to 3000 °C. The overall objective of this project is to establish a metrological infrastructure composed of reference facilities in order to provide industries and academic laboratories with traceable thermophysical properties data of any solid material up to 3000 °C.

Figure 1 shows a schematic representation of the diffusivimeter of LNE. The specimen (disk of 10 mm in diameter and 1 mm to 5 mm thick) is

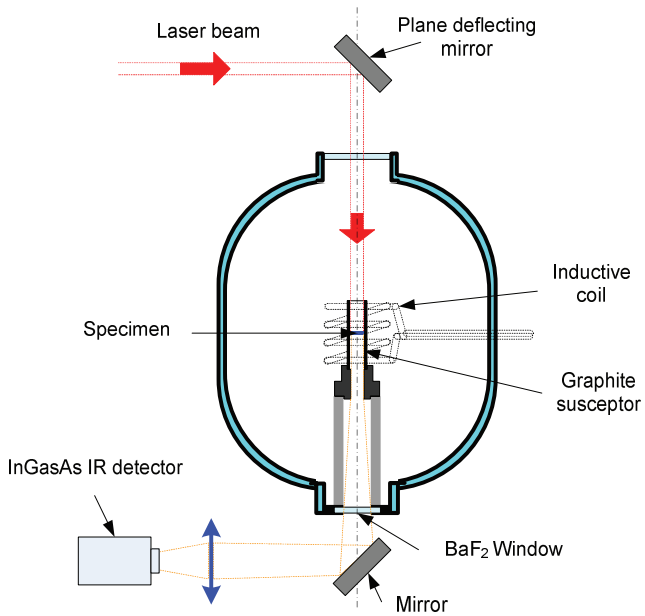

FIGURE 1
Schematic diagram of the diffusivimeter of LNE.

positioned inside an inductive furnace which is an airtight enclosure in the center of which an inductive coil and a movable susceptor are placed on a vertical axis. The inductor is a copper solenoid and the susceptor is a graphite hollow cylinder. The Foucault currents induced in the susceptor generate heat by Joule effect and the specimen located inside the susceptor is heated primarily by radiative transfer.

The temperature of the specimen is measured, once steady, with one of the two infrared bi-chromatic radiation thermometers used in function of the temperature level (cf. Table 2). The short thermal excitation is generated by a Nd:phosphate glass laser, whose beam is formed by a set of lenses and mirrors so that its diameter is about 10 mm on the front face of the specimen. The induced transient temperature rise of the specimen rear face is measured optically with infrared detectors installed with the radiation thermometers on the same linear translation stage enabling to put them opposite the 90° flat mirror attached below the susceptor.

Knowledge of the specimen temperature during test is a critical data required to ensure the relevance of the thermal diffusivity measurement and the associated uncertainty. Radiation thermometers can be subjected to drift over time and need thus to be periodically calibrated in order to ensure the accuracy of temperature measurements. The implementation of the laser flash method implies to take care of tricky optical alignments, between the laser beam and the front face of the specimen on the one hand, and between its rear face and the radiation thermometers and IR detectors on the other hand.

A slight misalignment of the radiation thermometer can indeed induce a significant error on the temperature measurement if the thermometer is not entirely centred on the specimen but is partially focused on a part of the susceptor close to the specimen.

For that reason, it is preferable to perform in-situ calibrations of the radiation thermometers instead of removing them out of the experimental facility for periodic calibrations. An in-situ calibration method of the radiation thermometers, adapted from studies performed in thermometry laboratories of some National Metrology Institutes [3], has been developed at LNE by using metal-carbon eutectic high temperature fixed points (HTFPs). HTFPs enable to generate repeatable and reproducible temperature levels in the range 1000 °C to 3000 °C using the melting/freezing of some eutectic metal-carbon alloys. Specific miniaturized high temperature fixed-point cell, filled with Pd-C (1492 °C), Pt-C (1738 °C), and Ir-C (2191 °C) [4] and suitable with the dimensions of the inductive furnace, have been implemented in this study in order to evaluate the feasibility of the proposed in-situ calibration method.

The principle of the method is to replace the specimen and the susceptor by a graphite crucible which contains a load of metal-carbon eutectic arranged at the bottom of a black-body cavity enabling the temperature measurement with the radiation thermometer to be calibrated.

This paper describes the design of the specific HTFP cells developed at LNE and suitable for the inductive furnace environment. The three metal-carbon eutectic alloys considered in this study have been characterized and made traceable to the ITS-90 [5] (International Temperature Scale of 1990) by assigning their freezing temperature from measurements performed with calibrated radiation thermometers. Results obtained through the experimental characterization of the specific fixed-point cells are presented and their metrological performances are discussed.

2 TECHNICAL FEATURES

2.1 Design of the metal-carbon eutectic high temperature fixed points

The HTFP cells are machined in a block of IG-510 high density graphite according to the dimensions of the graphite susceptor implemented in the inductive furnace. A black-body cavity (with a height of 38 mm and a diameter of 12 mm and whose bottom has an apex of 120°) is arranged on one side of the cells in order to enable temperature measurement with radiation thermometer. The other side of the cell, which contains the metal load, is not filled by a unique ingot but by series of metal rods. This configuration enables to easily fill in the crucible by introducing pure solid metal rods into wells with 1.5 up to 2 mm of diameter and 26 mm of height (*cf.* figure 2).

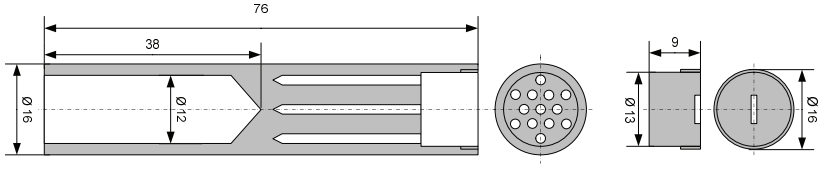

FIGURE 2
Cross-section of the HTFP crucible designed at LNE (main part of the cell and cap; dimensions in mm).

The amount of carbon required to obtain the binary alloy eutectic concentration is directly brought by the crucible. Considering the small size of the cell, it would have been tricky to obtain a homogeneous eutectic ingot (in terms of volume distribution of the metal load) if the cell had been filled from a powder mixture as usually done with larger radiometric and thermometric conventional HTFP cells. Solid metal rods enable to fill in efficiently all the available volume. Once the crucible has been filled, a graphite cap is screwed to seal the metal into the HTFP cell.

Two cells have been constructed for each metal-carbon eutectic alloy studied in order to perform reproducibility tests. Table 1 summarizes the main features of the HTFP cells tested.

TABLE 1
Characteristics of the HTFP cells and metal-carbon eutectic alloys

Metal	Purity	Eutectic carbon concentration (w%)	HTFP Temperature (°C)	Load mass (g)	
				Cell # 1	*Cell # 2*
Pd	3N5	2.7	1492	9.40	9.46
Pt	4N+	1.3	1738	17.00	16.48
Ir	3N	2.2	2291	17.71	17.81

2.2 Radiation thermometers

Temperature measurements are performed with two radiation thermometers in bi-chromatic mode only (two working wavelengths), this method having the advantage to be insensitive to the emissivity of the investigated surface in the respect of the grey body assumption.

The technical specifications of each radiation thermometer (RT) are summarized in table 2.

TABLE 2
Technical specifications of the bi-chromatic radiation thermometers

RT designation	Temperature range (°C)	Spectral bandwidth (µm)	Spot size (mm)
RT1800	700–1800	0.9 and 1.05	6
RT3000	1000–3000	0.9 and 1.05	3

Each radiation thermometer has been calibrated and made traceable to the ITS-90 by applying the two following methods:

- In the range 700 °C–1500 °C, the temperature calibration is performed by comparison to a standard black-body source. A correction on the black-body temperature is applied in order to take into account its emissivity in the effective spectral bandwidth of the radiation thermometer.
- In the range 1500 °C–3000 °C, calibration is performed by reference to a standard monochromatic radiation thermometer with a spectral bandwidth centred on 0.9 µm. Measured radiance temperature is corrected by the emissivity of the black-body cavity in order to compute the true temperature of the source which enables to calibrate the bi-chromatic radiation thermometer.

Calibration procedures have been applied with a BaF_2 window placed between the reference black-body cavities and the radiation thermometers

in order to have the same experimental conditions as in thermal diffusivity configuration. In addition to the calibration, the spot size has been controlled for each radiation thermometer at the focal working distance (50 cm). A variable size-aperture positioned in front of an uniform source (black body cavity) enabled to measure the spot sizes of the RTs as 6 mm and 3 mm for RT1800 and RT3000 respectively, in accordance with the manufacturer specifications which were given as 5.5 mm and 2.8 mm for these two RTs.

3 TEMPERATURE MEASUREMENT

3.1 Temperature homogeneity of the HTFP cavity

In a first step, a temperature profile is measured in the cavity of a HTFP cell out of the phase transition of the eutectic alloy by using the radiation thermometers. The furnace and HTFP cell being stabilized at 1670 °C, the spot of the radiation thermometer is centred in the cell cavity. Then the radiation thermometer is linearly translated in order to displace the spot along the cavity radius. Figure 3 illustrates the spot displacement in the cavity and the temperature profile obtained through this experiment.

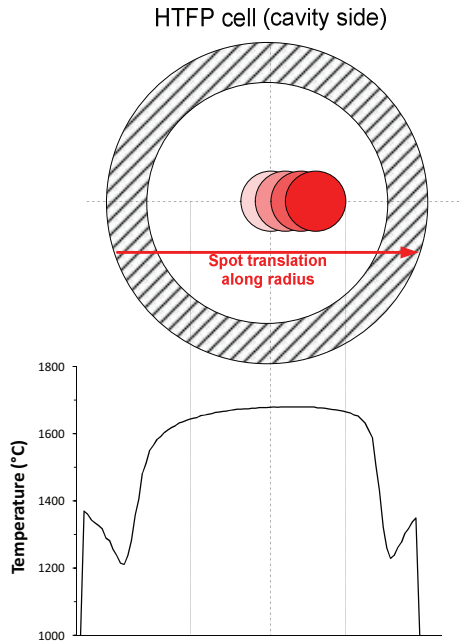

FIGURE 3
Measurement of the temperature profile in the HTFP cell cavity by RT 3000.

This test is repeated several times by removing and putting back the cell inside the furnace in order to evaluate the reproducibility of the optical alignment with the radiation thermometers. The spot-size has a significant influence on the temperature measurement. Since the results obtained with the RT 1800 maximize the uncertainty component, it is decided to apply also such values to the RT 3000 even if the consequence is an overemphasis of the global uncertainty in that case. It has been observed that the maximum error at 1670 °C due to the temperature gradient in the cell cavity and a misalignment of the radiation thermometer with the cavity centre is 6.82 °C. This error has to be taken into account in the uncertainty budget (cf. section 3.4). Calibration of the Pd-C HTFP cells (1492 °C)

In a second step, the three pairs of Pd-C, Pt-C and Ir-C HTFP cells have been successively calibrated in order to assign a freezing temperature traceable to the ITS-90 to each of them, by applying the following procedure.

The graphite susceptor is replaced by a HTFP cell in the inductive furnace (cf. figure 4), and is thermally stabilized at a temperature higher than the melting point of the metal carbon eutectic. The temperature of the furnace is then rapidly lowered to a temperature below the melting point by reducing the current in the inductive coil, causing thus the cooling of the HTFP cell down to a lower equilibrium temperature. In this configuration, the laser is disabled and the radiation thermometer spot is focused at the bottom of the cell cavity and measure the temperature of the HTFP during its cooling.

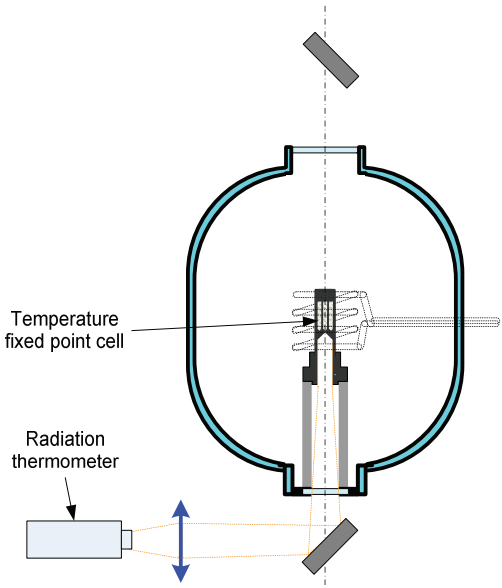

FIGURE 4
Radiation thermometer calibration by temperature fixed-point cell arrangement.

The thermal time response of the HTFP submitted to a variation of inductive heating is short. The small load of metal does not have a sufficient latent heat (compared to heat losses) to enable the radiation thermometer to observe a true flat melting plateau (Figure 5.a). Nonetheless, it is possible to detect a "freezing plateau" during the temperature drop as the freezing latent heat is high enough to generate a specific shape of the cooling curve. Figure 5.a presents a temperature versus time curve measured by the radiation thermometer RT1800 on the Pd-C cell #1 (identified Pd-C1) during the cooling process (red curve). The second derivative (blue curve) is computed from experimental smoothed data and is used to identify the freezing pattern and to assign a freezing temperature to the HTFP cell. The two successive zero-crossing observed with the second derivative enable to determine a time domain where the temperature drop is slowed down by the freezing of the eutectic. This time domain defines the "freezing plateau". The minimum value of the second derivative in this domain is correlated with the maximum temperature reached by the HTFP cell during the freezing process. Then, the fixed-point temperature is assigned from this singular point on the freezing plateau. The freezing temperature of this Pd-C cell has been measured during five successive freezing cycles performed on the same Pd-C cell and under the same thermal conditions with a repeatability of 0.12 °C (defined as the difference between the maximum and minimum measured values during the successive freezing cycles performed).

Figure 5.b demonstrates the sensitivity of the measured freezing temperature to the thermal conditions applied during the process. In these experiments, the HTFP cell is first thermally stabilized in liquid state over the melting temperature, then the power delivered by the inductive coil is adjusted in order to bring down the furnace to a final stabilized temperature which varies from one run to another in order to change the cooling thermal conditions. Since the cavity is not surrounded by the fixed-point material, the

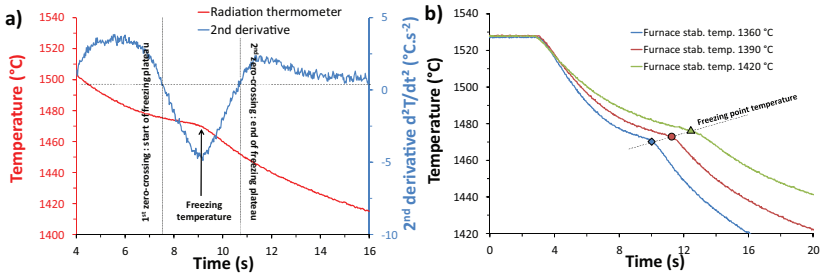

FIGURE 5
a) Typical freezing pattern measured with the Pd-C1 cell and freezing temperature determined by the second derivative method; b) Influence of the final stabilized temperature of the furnace on the Pd-C1 cell freezing temperature measured.

measurement is strongly influenced by the thermal exchanges between the cell and its environment: the lower the furnace temperature, the higher the radiative and conductive heat transfers from the cell to the surroundings. As a consequence, the apparent freezing temperature measured by the radiation thermometer is shifted down from the expected level, and the obtained value depends on the final stabilized furnace temperature.

A specific extrapolation procedure [6, 7] has been thus used to eliminate the influence of the temperature drop speed. Series of freezing "plateau" have been measured on the same HTFP cell by keeping constant the initial temperature of the furnace and by changing its final stabilization temperature. Figure 6 shows the measurement series obtained using the radiation thermometers RT1800 (a) and RT3000 (b) with the same Pd-C1 cell, where the measured freezing temperatures are plotted as a function of the furnace final stabilized temperature. The dashed line represents the ideal adiabatic condition, obtained if the furnace is at the thermal equilibrium with the HTFP cell and the metal-carbon eutectic under freezing. Practically, adiabatic line is plotted as the set of points where the freezing temperature is equal to the furnace stabilized temperature. The true freezing temperature of the Pd-C1 cell is determined by the intersection point between the extrapolation of the linear fit computed on the experimental data and the "ideal adiabatic conditions" line. At this stage, the calibration error of the radiation thermometers (determined according to the two methods described in section 2.2) is not corrected.

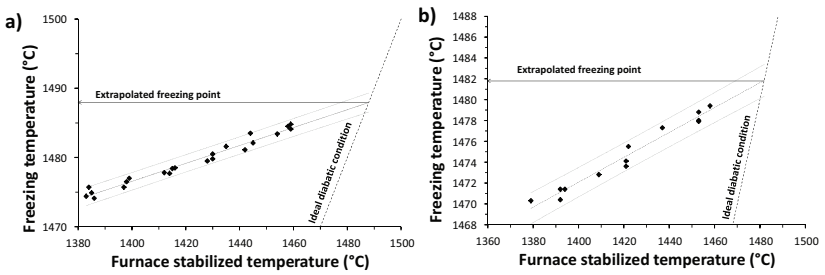

FIGURE 6
Extrapolated value of the Pd-C1 cell freezing point temperature determined using the radiation thermometers RT1800 (a) and RT3000 (b) before correction.

A freezing temperature traceable to the ITS-90 can be assigned to the two Pd-C cells by applying the appropriate calibration corrections on extrapolated freezing temperatures measured by each radiation thermometer. Results are summarized in table 3.

Measurement series presented here have been performed before and after a maintenance operation on the furnace (change of the inductive coil and cleaning of the internal wall of the furnace).

TABLE 3
Freezing temperature assigned to the Pd-C cells from measurements performed with each calibrated radiation thermometer

RT designation	Pd-C cell #	Extrapolated temperature (°C)	Calibration correction (°C)	Assigned temperature (°C)	RT calibration uncertainty k = 2 (°C)
RT1800	1	1487.94	7.16	1495.10	4.40
	1	1499.94(*)		1507.10(*)	
	2	1488.17		1495.33	
RT3000	1	1481.89	9.76	1491.65	4.58
	1	1492.22(*)		1501.98(*)	
	2	1493.30(*)		1503.06(*)	

(*) Measurements performed after maintenance operation on the furnace

A change of the freezing temperature result is observed for the cell n°1 of Pd-C between measurements performed before and after the maintenance operation of the furnace (disassembly, cleaning and reassembly of the furnace and the inductive coil). This observation being the same for the two pyrometers, it is due more to a modification of the temperature gradient inside the furnace (induced by the maintenance operation) than to an unlikely similar drift of the two instruments. The change of the temperature profile along the fixed-point cell height affects indeed the apparent temperature of the cell.

3.2 Calibration of the Pt-C (1738 °C) and Ir-C (2291 °C) fixed-point cells

Pt-C and Ir-C cells were implemented and studied in the inductive furnace by following the same experimental procedures as the one applied with the Pd-C HTFP cells.

Figure 7.a shows three freezing plateaus observed with the Pt-C1 cell, and Figure 7.b illustrates the extrapolation method applied to the measurement series obtained with the RT1800 and RT3000 radiation thermometers.

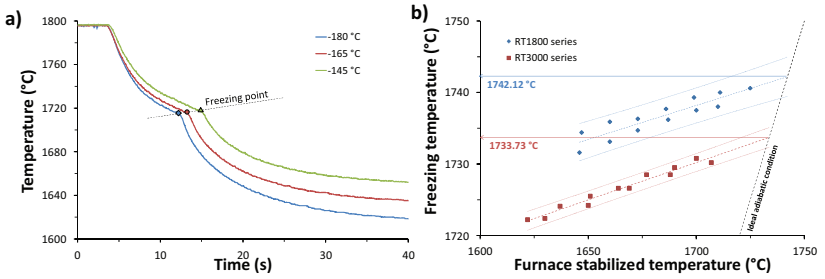

FIGURE 7
a) Freezing plateaus observed with the Pt-C1 cell implemented under different final thermal conditions; b) Extrapolated freezing temperatures measured on Pt-C1 cell with both RT1800 and RT3000 thermometers (without calibration corrections).

The repeatability obtained by performing five successive freezing plateaus on the Pt-C1 cell under the same thermal conditions is 0.85 °C with RT1800 and 0.58 °C with RT3000.

The freezing temperatures (traceable to the ITS-90), assigned to each Pt-C cell from measurements performed with the two calibrated radiation thermometers, are summarized in table 4.

TABLE 4
Freezing temperature assigned to the Pt-C cells from measurements performed with each calibrated radiation thermometer

RT designation	Pt-C cell #	Extrapolated temperature (°C)	Calibration correction (°C)	Assigned temperature (°C)	RT calibration uncertainty k = 2 (°C)
RT1800	1	1742.12	9.46	1751.58	5.54
	2(*)	1748.44(*)		1757.90(*)	
RT3000	1	1733.73	14.6	1748.33	6.32
	2(*)	1750.83(*)		1765.43(*)	

(*) Measurements performed after maintenance operation on the furnace

A metallic leakage has been observed at the cavity bottom of the Pt-C1 cell after the first measurement series. Only the Pt-C2 cell was implemented after the maintenance operation performed on the inductive furnace. Contrariwise to the other fixed-point cells tested in this study, it was consequently not possible to evaluate the two-cell reproducibility. In order to evaluate the uncertainty component due to the two-cell reproducibility that is integrated in the uncertainty budget presented in section 3.4 for the Pt-C fixed-point, it has been decided to interpolate the standard corresponding uncertainty component from the values assessed at the Pd-C and Ir-C freezing temperatures by assuming a linear variation.

Freezing temperature measurements were performed on the Ir-C cells with the RT3000 only, because the RT1800 was out of range at this temperature level.

Figures 8.a shows three freezing plateaus observed with the Ir-C1 cell implemented under different cooling conditions. Figures 8.b illustrates the extrapolation of the Ir-C1 cell freezing temperature for an ideal adiabatic condition.

The repeatability obtained by performing five successive freezing plateaus on the Ir-C1 cell under the same thermal conditions with RT3000 is 1.27 °C.

The freezing temperatures (traceable to the ITS-90) assigned to each Ir-C cell from measurements performed with the calibrated RT3000 radiation thermometer are summarized in table 5.

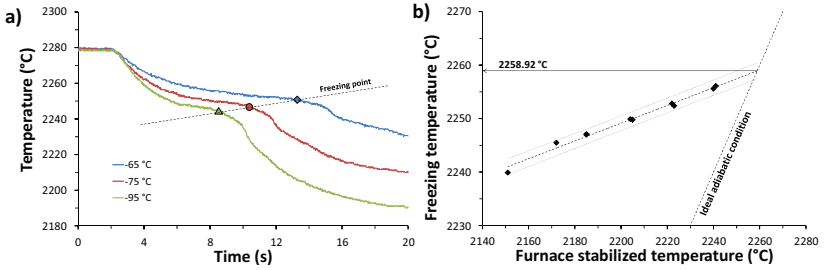

FIGURE 8
a) Freezing plateaus observed with the Ir-C1 cell implemented under different final thermal conditions; b) Extrapolated freezing temperatures measured on Ir-C1 cell with the RT3000 thermometer (without calibration correction).

TABLE 5
Freezing temperature assigned to the Ir-C cells from measurements performed with the RT3000 calibrated radiation thermometer

Ir-C cell #	Extrapolated temperature (°C)	Calibration correction (°C)	Assigned temperature (°C)	RT calibration uncertainty k = 2 (°C)
1	2258.92	29.57	2288.49	10.33
1	2270.55(*)		2300.12(*)	
2	2273.35(*)		2302.92(*)	

(*) Measurements performed after maintenance operation on the furnace

3.3 Uncertainties

An uncertainties budget associated to the assignment of a freezing temperature to this first set of HTFP cells has been established. The main uncertainty components are listed below:

- RT calibration: Uncertainty due to the two procedures described in 2.3 for the calibration of the radiation thermometer.
- RT resolution: Uncertainty associated to the temperature resolution of the radiation thermometer.
- RT alignment: Uncertainty associated to the optical alignment of the radiation thermometer with the centre of the HTFP cell cavity (cf. section 3.1). The temperature profile of the HTFP cell cavity measured at 1670 °C is extrapolated to the other temperature levels by assuming a proportional variation of the temperature gradient. Such coefficient is computed as the ratio between the reference temperature (1670 °C) and the temperature level which corresponds to the considered fixed-point.
- Cell repeatability: Uncertainty associated to the repeatability of the cell freezing temperature obtained by performing five successive freezing

plateaus under the same thermal conditions (i.e same cooling conditions of the furnace) on a same cell. Corresponding standard uncertainty is computed as the half value of the maximum deviation of the five freezing temperatures obtained.

- Two-cell reproducibility: Uncertainty associated to the reproducibility of the freezing temperatures measured on a couple of HTFP cells with the same radiation thermometer under the same thermal conditions. Corresponding standard uncertainty is computed as the half value of the deviation between the freezing temperatures measured on the two cells.
- Extrapolation Model: Uncertainty due to the error associated to the linear fit applied on measurement series for the extrapolation of the freezing temperature under ideal adiabatic conditions.
- Thermal conditions reproducibility: Uncertainty due to the thermal conditions in the furnace, quantified as the effective difference between the temperatures measured on a same cell before and after the maintenance operation performed on the furnace.

Table 6 details the uncertainty budget assessed for the assignment of a freezing temperature to the Pd-C1 cell with the RT1800 radiation thermometer. The uncertainty budgets are given for the freezing temperatures assigned to Pt-C1 and Ir-C1 cells from measurements performed with the RT3000 radiation thermometer.

The freezing temperatures measured and assigned to each cell tested in this study are summarized in Table 7 with their associated expanded uncertainties. This data set is also plotted in Figure 9.

These results show the high sensitivity of the freezing temperature measurement to the thermal conditions around the HTFP cells in the furnace. As explained in § 3.2, the apparent drifts observed for the Pd-C and the Pt-C freezing temperatures with the two pyrometers are ascribed to a measurement bias linked to a variation of the thermal conditions (i.e temperature profile along the HTFP cells) rather than to a simultaneous drift of the two instruments which is much less probable.

As it is shown in figure 9, measurements performed on Pd-C and Ir-C freezing points before the maintenance operation (when the position of the HTFP cells in the furnace was optimum relatively to the temperature profile inside the inductive coil) are in good agreement with the targeted values (1492 °C and 2291 °C respectively), the differences between the obtained data and the targeted values being within the expanded uncertainties given in Table 7.

The measured freezing temperatures of the Pt-C cells appear overestimated compared to the expected value (1738 °C). This overestimation being observed with the two radiation thermometers for the two Pt-C cells, it could be explained by a bias introduced by eutectic alloy due to a chemical contamination of the platinum used for filling the crucible and/or heterogeneous carbon concentration.

TABLE 6
Uncertainty budgets associated to the assignment of a freezing temperature respectively to Pd-C1 cell using the RT1800 radiation thermometer, and to Pt-C1 and Ir-C1 cells using the RT3000 radiation thermometer

Pd-C1 cell				
Quantity	**Standard uncertainty (°C)**	**Probability distribution**	**Sensitivity coefficient**	**Contribution to the uncertainty k = 1 (°C)**
RT calibration	2.20	*Normal*	1	2.20
RT resolution	0.06	*rectangular*	1	0.06
RT alignment	3.50	*Rectangular*	0.89	3.12
Cell repeatability	0.06	*Normal*	1	0.06
2-cells reproducibility	0.12	*Normal*	1	0.12
Extrapolation model	1.38	*Normal*	1	1.38
Thermal conditions	6.93	*Rectangular*	1	6.93
	Combined uncertainty k = 1 (°C)			8.03
	Expanded uncertainty k = 2 (°C)			**16.06**
Pt-C1 cell				
Quantity	**Standard uncertainty (°C)**	**Probability distribution**	**Sensitivity coefficient**	**Contribution to the uncertainty k = 1 (°C)**
RT calibration	3.16	*Normal*	1	3.16
RT resolution	0.06	*rectangular*	1	0.06
RT alignment	3.94	*Rectangular*	1.04	4.10
Cell repeatability	0.29	*Normal*	1	0.64
2-cells reproducibility[(a)]	0.85	*Normal*	1	0.85
Extrapolation model	1.38	*Normal*	1	1.38
Thermal conditions	9.87	*Rectangular*	1	9.87
	Combined uncertainty k = 1 (°C)			11.28
	Expanded uncertainty k = 2 (°C)			**22.56**
Ir-C1 cell				
Quantity	**Standard uncertainty (°C)**	**Probability distribution**	**Sensitivity coefficient**	**Contribution to the uncertainty k = 1 (°C)**
RT calibration	5.17	*Normal*	1	5.17
RT resolution	0.06	*rectangular*	1	0.06
RT alignment	3.94	*Rectangular*	1.37	5.40
Cell repeatability	0.64	*Normal*	1	0.64
2-cells reproducibility	1.40	*Normal*	1	1.40
Extrapolation model	1.50	*Normal*	1	1.50
Thermal conditions	6.72	*Rectangular*	1	6.72
	Combined uncertainty k = 1 (°C)			10.28
	Expanded uncertainty k = 2 (°C)			**20.56**

(a) Interpolated value by assuming a linear variation of the reproducibility between the Pd-C and Ir-C freezing temperatures.

TABLE 7
Freezing temperatures assigned to each HTFP cell with associated expanded uncertainties

Radiation thermometer	HTFP eutectic	Cell designation	Freezing temperature (°C)	Expanded uncertainty k = 2 (°C)
RT1800	Pd-C	1	1495.10	16.06
		2	1495.33	16.02
		1	1507.10(*)	16.17
	Pt-C	1	1751.58	18.55
		2	1757.90 (*)	18.95
RT3000	Pd-C	1	1491.65	14.58
		1	1501.98 (*)	14.85
		2	1503.06 (*)	14.49
	Pt-C	1	1748.33	22.56
		2	1765.43 (*)	22.97
	Ir-C	1	2288.49	20.56
		1	2300.12 (*)	20.15
		2	2302.92 (*)	20.63

(*)Measurements performed after maintenance operation on the furnace

Measurement series performed on the three eutectic alloys have demonstrated that it is possible to check periodically an eventual drift of the radiation thermometers by considering the reproducibility and repeatability properties observed on the freezing point of HTFP cells positioned in a stable temperature profile.

The expanded uncertainty levels (assessed to be between 15 °C and 20 °C approximately) associated to the assignment of freezing temperatures to the three HTFP cells (Pd-C Pt-C and Ir-C) developed here are suitable with the in-situ calibration of infrared thermometers used for thermal diffusivity measurements at high temperature. Thermal diffusivity measurements performed by LNE on isostatic graphite and tungsten specimens up to 2000 °C in a previous study [8] have indeed shown that the sensitivity of thermal diffusivity to temperature decreases progressively when the temperature increases and that a 20 °C variation on the specimen temperature generates an additional component of relative uncertainty lower than 0.7 % on the thermal diffusivity measurement for these two materials. The contribution of the uncertainty component due to the radiation thermometer calibration is relatively low compared to the overall expanded uncertainty associated with thermal diffusivity measurements which was evaluated to be equal to around 5.5 % [9] for thermal diffusivity measurements performed at these temperature levels. Preliminary results obtained recently by LNE on graphite

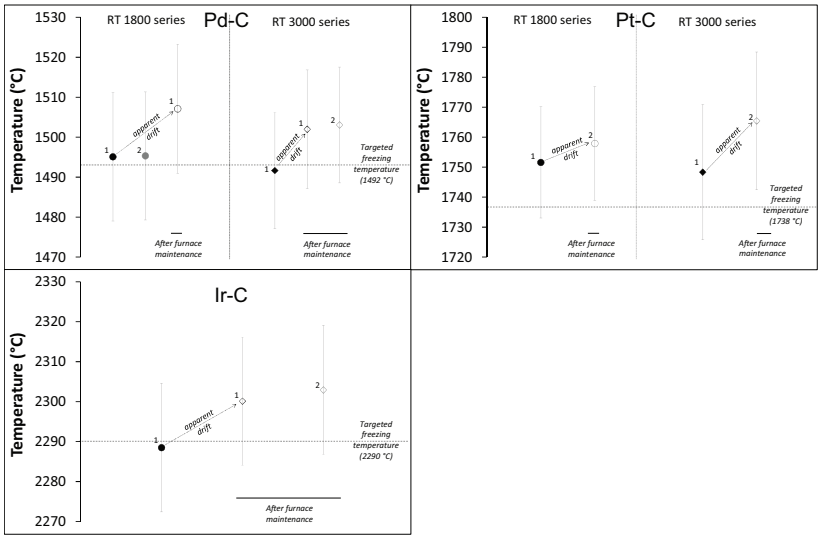

FIGURE 9
Freezing temperatures assigned to each HTFP couples of cells with associated expanded uncertainties, from measurement series performed with the two radiation thermometers before and after the maintenance operation on the inductive furnace.

specimens in the temperature range from 2000 °C to 3000 °C in the frame of the Hi-TRACE project seem to confirm this behaviour.

4 CONCLUSION AND FUTURE DEVELOPMENTS

A set of six high temperature fixed-point cells has been specifically designed and constructed at LNE to be implemented in the inductive furnace of a diffusivimeter. Three binaries metal-carbon eutectic alloys (Pd-C, Pt-C, Ir-C) have been characterized regarding their ability to generate controlled and reproducible freezing temperatures, using two radiation thermometers previously calibrated and made traceable to the ITS-90.

The experiments have demonstrated the relevance of such a method to control and correct the potential drift of the radiation thermometers along time. Indeed, the freezing points have shown acceptable characteristics in terms of repeatability and reproducibly, which justify their use as candidate reference devices to generate quite stable and reliable temperature level.

The specific thermal conditions within an inductive furnace have shown the limitations of such HTFP cells design. The metal distribution along the height of the cell is not an appropriate configuration taking into account the limited homogeneous temperature area generated by the inductive coil (about one centimetre in height). Consequently, the measured freezing temperature

on such HTFP cells is strongly affected by the temperature profile within the furnace. In order to improve the reproducibility of the freezing temperature and to minimize the influence of the cell positioning into the furnace, it is envisaged to design a new miniature HTFP cell generation. The next crucibles should have a limited height (no more than one centimetre) with suppression of the cavity, in order that the eutectic metal-carbon ingots will be located in the homogeneous area of the temperature profile generated by the inductive furnace.

The new HTFP cells will look like thermal diffusivity specimens (cylinder with a diameter of 10 to 12 mm), the radiation thermometers will be thus focused on a planar surface instead of the bottom of a black body cavity (as in the current HTFP cells). It should be possible to optimize the thermal conditions of the metallic load during its phase change in order to improve the "signatures" of freezing plateau, and to obtain melting curves which would enable to optimize the thermal correction method by defining a fixed-point temperature free from environmental thermal influences with a lower level of uncertainty. These developments will be done at LNE in the second part of the Hi-TRACE project.

ACKNOWLEDGEMENTS

This work is funded through the European Metrology Programme for Innovation and Research (EMPIR) Project "17IND11 – Hi-Trace". The EMPIR is co-financed by the Participating States and from the European Union's Horizon 2020 research and innovation programme.

REFERENCES

[1] W.J. Parker, R.J. Jenkins and G.L. Abbott, *J. Appl. Phys*., vol. 32 (1961), 1679-1684, https://doi.org/10.1063/1.1728417.
[2] K. Boboridis, B. Hay, *ATW-Int J Nucl Power*, **65**, n°3 (2020), 140, ISSN 1431-5254.
[3] G. Machin, "Twelve years of high temperature fixed point research: a review", *AIP Conf. Proc.,* **1552** (2013), 305-316, https://doi.org/10.1063/1.4821383.
[4] Guide on secondary thermometry, *Comité Consultatif de thermométrie*, BIPM (2018) https://www.bipm.org/utils/common/pdf/ITS-90/Specialized-FPs-above-0C.pdf.
[5] H. Preston-Thomas, *Metrologia*, **36** (1990), 3-10, https://doi.org/10.1088/0026-1394/27/1/002.
[6] O. Ongrai, J.V. Pearce, G. Machin, S.J. Sweeney, *Meas. Sci. Technol.,* **22** (2011), 1-7, https://doi.org/10.1088/0957-0233/22/1/015104.
[7] G. Failleau, C.J. Elliott, T. Deuzé, J.V. Pearce, G. Machin, M. Sadli, *Int. J. Thermophys.,* **35** (2014), 1223–1238, https://doi.org/10.1007/s10765-014-1667-4.
[8] B. Hay, K. Anhalt, L. Chapman, K. Boboridis, J. Hameury, S. Krenek, L. Vlahovic, N. Fleurence, O. Beneš, *IEEE Transactions on Nuclear Sciences,* **61**:4 (2014), 2112-2119, https://doi.org/10.1109/TNS.2014.2300552.
[9] B. Hay, J.R. Filtz, J. Hameury, L. Rongione, *Revue Française de Métrologie,* **14**, Vol. 2008-2 (2008), 3-11, ISSN 1772-1792.